Guar gum solutions for improved delivery of iron particles in porous media (Part 2): Iron transport tests and modeling in radial geometry

Guar gum solutions for improved delivery of iron particles in porous media (Part 2): iron transport tests and modelling in radial geometry

Supporting Information

Journal of Contaminant Hydrology

June 2014

Tiziana Tosco[(1)], Francesca Gastone[(1)], Rajandrea Sethi[(1)*]

[(1)] DIATI – Dipartimento di Ingegneria dell'Ambiente, del Territorio e delle Infrastrutture – Politecnico di Torino, C.so Duca degli Abruzzi 24, 10129 Torino, Italy

[*] Corresponding Author: phone +39 (011) 564 7735; e-mail: rajandrea.sethi@polito.it

Index

1. Derivation of sedimentation kinetics in horizontal columns

The formulation of the removal kinetics due to sedimentation for transport and retention of particles in porous media, in case of horizontal flow (1D Cartesian coordinates) can be derived as follows.

Let us consider a horizontal pore of length L, vertical cross section A_v, horizontal cross section A_h, average size $d_{50,sand}$. The horizontal cross section can be expressed as a function of the average pore size:

$$A_h = \varphi L d_{50,sand} \qquad \textbf{(S 1)}$$

where φ [-] is a shape factor depending on the geometry of the pore.

The volume of the pore is then:

$$V_{pore} = \varphi' L d_{50,sand}^2 \qquad \textbf{(S 2)}$$

where φ' [-] is another shape factor. For cylindrical pores, $\varphi' = \pi/4$.

Particles suspended in the pore fluid are transported through it by a horizontal flow with effective flow rate v_e. The particles have a size $d_{50,Fe}$ (eg. iron particles), known sedimentation rate v_s (eg. derived from Stokes law, or modified Stokes law for non Newtonian fluids, or measured). The process is summarized in Figure S. 1.

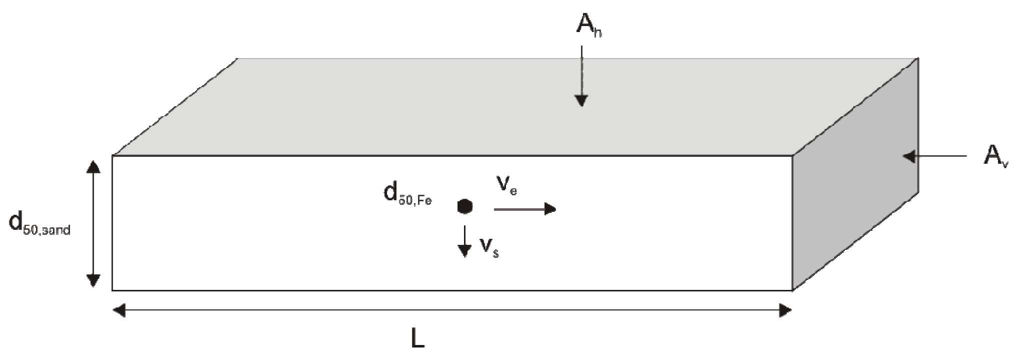

Figure S. 1: Scheme of particle transport and sedimentation in a horizontal pore

The sedimentation rate v_s is supposed to be constant. Under the hypothesis of particles homogeneously dispersed in the pore fluid, the average sedimentation path, L_s, is equal to half the vertical size of the pore, $d_{50,sand}/2$.

The mass flux of sedimenting particles at the center of the pore (maximum horizontal section), J_s [M T^{-1}], is:

$$J_s = A_h v_s c_{Fe} = \varphi L d_{50,sand} v_s c_{Fe} \qquad \textbf{(S 3)}$$

Up-scaling from the single pore to the porous medium with porosity ε leads to a corresponding volume of porous medium V_{pm} equal to:

$$V_{pm} = \varphi' \frac{1}{\varepsilon} L d_{50,sand}^2 \qquad \textbf{(S 4)}$$

As a consequence, the mass flux of sedimenting particles per unit mass of porous medium, J_s/V_{pm} [M L^{-3} T^{-1}] is:

$$\frac{J_s}{V_{pm}} = \varepsilon \frac{\varphi L d_{50,sand} v_s c_{Fe}}{\varphi' L d_{50,sand}^2} = \varepsilon C_a \frac{v_s}{d_{50,sand}} c_{Fe} \qquad \textbf{(S 5)}$$

where C_a is a coefficient resulting from the combination of the previously introduced shape factors.

The normalized mass flux J_s/V_{pm} is also equivalent to the term expressing the removal of particles from the fluid phase in the mass balance equation for particle transport through a porous medium:

$$\frac{\partial}{\partial t}(\varepsilon c_{Fe}) + \frac{\partial(\rho_b s_{Fe})}{\partial t} + \frac{\partial}{\partial x}(q c_{Fe}) - \frac{\partial}{\partial x}\left(\varepsilon D \frac{\partial c_{Fe}}{\partial x}\right) = 0 \qquad \textbf{(S 6)}$$

where

$$\frac{\partial(\rho_b s_{Fe})}{\partial t} = \frac{J_s}{V_{pm}} \qquad \textbf{(S 7)}$$

As a consequence, the kinetics of the irreversible removal of particle due to sedimentation is a first-order kinetics with deposition rate k_a proportional to the ratio of sedimentation rate to pore size diameter:

$$\frac{\partial(\rho_b s_{Fe})}{\partial t} = \varepsilon k_a c_{Fe} = \varepsilon C_a \frac{v_s}{d_{50,sand}} c_{Fe} \qquad \textbf{(S 8)}$$

where

$$k_a = C_a \frac{v_s}{d_{50,sand}} \qquad \textbf{(S 9)}$$

If the amount of particles deposited is relevant and modifies the volume and shape of the pores, the term $C_a/d_{50,sand}$ is not constant, and decreases with increasing the concentration of deposited particles. This variation is modelled in this work implementing the formulation for clogging processes previously developed by the authors [*Tosco and Sethi*, 2010]:

$$\frac{\partial(\rho_b s_{Fe})}{\partial t} = \varepsilon k_a c_{Fe} = \varepsilon C_a \frac{v_s}{d_{50,sand}}\left(1 + A s_{Fe}^B\right)c_{Fe} \qquad \textbf{(S 10)}$$

The formulation of equation S8 is equivalent to the one obtained applying the clean bed filtration theory, provided that the sedimentation is assumed as the unique removal mechanism, and the formulation of Yao is adopted:

$$\eta_0 = \eta_G = \frac{v_s}{v_e} \qquad \textbf{(S 11)}$$

The formulation of equation S8 is equivalent to the one obtained applying the clean bed filtration theory, provided that the sedimentation is assumed as the unique removal mechanism, and the formulation of Yao is adopted:

$$\frac{\partial(\rho_b s_{Fe})}{\partial t} = \varepsilon \frac{3}{2}(1-\varepsilon)\frac{v_e}{d_{50,sand}} \alpha_{att} \eta_G c_{Fe} \qquad \textbf{(S 12)}$$

If equation S11 is substituted in S12, the removal rate k_a becomes:

$$k_a = \frac{3}{2}(1-\varepsilon)\frac{v_e}{d_{50,sand}} \alpha_{att} \qquad \textbf{(S 13)}$$

which compared to equation S9 leads to:

$$C_a = \frac{3}{2}(1-\varepsilon)\alpha_{att} \qquad \textbf{(S 14)}$$

2. **Matlab script for decorrelation of susceptibility profiles**

```
% Decorrelation function for susceptometer data
% REFERENCE:
% TOSCO T., GASTONE F., SETHI R. (2014). Guar gum solutions for improved
% delivery of iron particles in porous media (Part 2): iron transport tests and
% modelling in radial geometry, JOURNAL OF CONTAMINANT HYDROLOGY
% Developed by Rajandrea Sethi, DIATI Politecnico di Torino,
% rajandrea.sethi@polito.it

% DATA matrix (example):
% 1st column: x along column
% 2nd column and following: K1 K2 .... KN (each K column represents a measured
profile)
xd=[
0   1   1   747 408 392;
2   -1  -1  738 451 439;
4   -2  -1  668 434 413;
6   -2  -2  604 413 391;
8   -2  -1  580 402 396;
10  -2  -2  562 368 390;
12  -2  -2  524 312 344;
14  -3  -2  516 293 323;
16  -2  -2  509 282 305;
18  -1  -2  496 270 288;
20  -1  -1  464 233 248;
22  -1  -1  424 187 193;
24  -2  -2  397 163 161;
26  -2  -1  385 157 144;
28  -2  -1  373 140 133;
30  -1  -2  370 129 124;
32  -2  -2  355 122 109;
34  -2  -1  345 118 98;
36  -1  -2  335 112 83;
38  -2  -2  328 104 77;
40  -2  -2  320 90  74;
42  2   3   299 75  71]


% Bartington Susceptometer weight function: Length Krel
% 1st column is space position
% 2nd column is weight function
yd=[
-4.366818031    0.015206463;
-4.091669774    0.020445565;
-3.85179475 0.025693079;
-3.576645958    0.030932181;
-3.16743784 0.04321293;
-2.934612712    0.050230783;
-2.715886304    0.060789182;
-2.412493884    0.074864199;
-2.250205613    0.085436271;
-2.094971774    0.096010053;
-1.93266775 0.111887883;
-1.643334006    0.143651955;
-1.495103875    0.171913083;
-1.339799022    0.207246622;
-1.205648392    0.24612255;
-1.120870251    0.288547569;
-1.029042749    0.329202383;
-0.951288606    0.382240493;
```

```
-0.859374873    0.452960823;
-0.816924933    0.495396097;
-0.78151928 0.541370207;
-0.739069341    0.583805347;
-0.710774453    0.610327034;
-0.675394698    0.647458259;
-0.632919396    0.698736418;
-0.59052018 0.723486055;
-0.55513989 0.76061728;
-0.505671024    0.790670967;
-0.477381209    0.815424022;
-0.279540184    0.923258485;
-0.223036641    0.946236073;
-0.152418625    0.970978874;
-0.095940444    0.98511371;
-0.039472408    0.995711419;
0   1;
0.039472408 0.995711419;
0.095940444 0.98511371;
0.152418625 0.970978874;
0.223036641 0.946236073;
0.279540184 0.923258485;
0.477381209 0.815424022;
0.505671024 0.790670967;
0.55513989  0.76061728;
0.59052018  0.723486055;
0.632919396 0.698736418;
0.675394698 0.647458259;
0.710774453 0.610327034;
0.739069341 0.583805347;
0.78151928  0.541370207;
0.816924933 0.495396097;
0.859374873 0.452960823;
0.951288606 0.382240493;
1.029042749 0.329202383;
1.120870251 0.288547569;
1.205648392 0.24612255;
1.339799022 0.207246622;
1.495103875 0.171913083;
1.643334006 0.143651955;
1.93266775  0.111887883;
2.094971774 0.096010053;
2.250205613 0.085436271;
2.412493884 0.074864199;
2.715886304 0.060789182;
2.934612712 0.050230783;
3.16743784  0.04321293;
3.576645958 0.030932181;
3.85179475  0.025693079;
4.091669774 0.020445565;
4.366818031 0.015206463]

% sorts the weight function, in case it was measured:
yd=sortrows([-yd(:,1),yd(:,2)])
xd_int=sort([-xd(2:length(xd)) xd(:,1)'])
y=interp1(yd(:,1),yd(:,2), xd_int, 'linear',0)
[n,co]=size(xd);

% Decorrelation:
A=[];
for i=1:n
    A=[A; y(n+1-i:2*n-i)]
```

```
end
x_dec=[]
for i=2:co
    x2=A\xd(:,i)
x_dec=[x_dec x2];
end


% Final plot

figure(1)
subplot(2,1,1)
plot(xd(:,1),x_dec); title('After decorrelation')
subplot(2,1,2)
plot(xd(:,1),xd(:,2:co)); title('Before decorrelation')
```

3. References

Logan, B. E., D. G. Jewett, R. G. Arnold, E. J. Bouwer, and C. R. O'Melia (1995), Clarification of clean-bed filtration models, *Journal of Environmental Engineering*, *121*(12), 869-873.

Tosco, T., and R. Sethi (2010), Transport of non-newtonian suspensions of highly concentrated micro- and nanoscale iron particles in porous media: A modeling approach, *Environmental Science and Technology*, *44*(23), 9062-9068.

Yao, K.-M., M. T. Habibian, and C. R. O'Melia (1971), Water and waste water filtration. Concepts and applications, *Environmental Science & Technology*, *5*(11), 1105-1112.